Text and references accompanying Nevada Bureau of Mines and Geology Open-File Report 19-3

Geologic Map of the Independence Valley NW Quadrangle, Elko County, Nevada

by

Andrew V. Zuza[1], Seth Dee[1], Christopher D. Henry[1], Michael W. Ressel[1], and Charles H. Thorman[2]

[1]Nevada Bureau of Mines and Geology, University of Nevada, Reno
[2]U.S. Geological Survey, Emeritus, Denver, CO

2019

Disclaimer: NBMG open-file reports are preliminary. They have not been thoroughly edited or peer reviewed. This geologic map was funded in part by the USGS National Cooperative Geologic Mapping Program under STATEMAP award number G18AC00198, 2019 and G16AC00186, 2017.

GEOLOGIC UNITS

Quaternary Deposits

Qa Active Alluvium (Holocene) Coarse-grained alluvial deposits in incised ephemeral drainages; typically unconsolidated and poorly to moderately sorted sand with pebble- to cobble-sized gravel. Locally forms low terraces above active drainages. Minimal soil development. Correlative with young alluvial-fan deposits (Qfy).

Qfy Young alluvial-fan deposits (Holocene) Coarse-grained alluvial deposits in intermittently active alluvial-fans; typically sandy, pebble- to cobble-sized gravel with silt and boulders; some localized areas primarily comprised of silt with minimal coarse-grained material. Clasts are subrounded to subangular. Surfaces have distributary flow patterns with morphology ranging from subdued bar-and-channel forms to slightly smoothed surfaces. Typically has weak to no soil development. If present, soil development is characterized by Stage I, $CaCO_3$ coatings on bottoms of clasts. The distal margins of Qfy fans are commonly buttressed against beach bars of lacustrine gravels (Qlg). Exposed thickness of the unit is typically 1–2 m. Areas of high silt composition are isolated from the major drainage outlets, or deposited beyond the distal edge of gravel deposition. The silt-rich fans are comprised of reworked fine-grained sediments that were initially deposited by a pre-late Pleistocene lake in the Independence Valley (Reheis, 1999).

Qe Eolian sand (Holocene) Light brown, well-sorted, fine- to medium-grained sand deposits buttressed adjacent to the west side of Qlg beach bars. Commonly forms barchan dunes with asymmetries suggesting prevailing winds out of the east-northeast.

Qgwd Ground water discharge deposits (Holocene) Deposits of eolian and alluvial, sand and silt with organic clay, in heavily vegetated area surrounding active discharging springs. Includes spring, spring mounds, ponds, wet meadows and seasonally flowing spring-fed streams.

Qpa Playa and alluvial deposits (Holocene) Fine-grained deposit in the nearly flat axis of Independence Valley; typically light gray to grayish brown silt, clay and minor fine sand. Deposited during inundation of the playa with shallow standing water. Sediments include evaporite deposits and efflorescent salt crusts. Surface has sufficient gradient that playa deposits are locally reworked in shallow gullies. Interfingers with, and locally overlain by, Qgwd deposits.

Qla Lacustrine and alluvial deposits (Holocene to late Pleistocene) Variable deposits of lacustrine silt, clay and sand; and alluvial silt, sand and minor gravel. Lacustrine silt was deposited in shallow waters of late Pleistocene Lake Clover, which had highstands at approximately 19.5 ka and 17.0 ka (Munroe and Laabs, 2013). Alluvial deposits are present in channels and are comprised of reworked lacustrine deposits and distal fan sediments.

Qlg Lacustrine gravels (late Pleistocene) Gray to brown deposits of moderately to well sorted pebble- to cobble-sized gravel and sand in shorelines, beach bars, and spits. Clasts are rounded to subrounded. Soils consist of 20- to 30-cm thick Bw horizon, underlain by 30–50 cm stage II $CaCO_3$ horizons (Bk). Snail shells are common. Unit was deposited during highstands and regressive phases of late Pleistocene Lake Clover. Lake Clover reached a maximum elevation of 1729 m at 19.5 ka and 17.0 ka (Munroe and Laabs, 2013). Qlg shoreline deposits are inset into Qfi fan deposits. Exposed thickness of unit is 3+ m.

Qfi Intermediate-aged alluvial-fan deposits (late Pleistocene) Coarse-grained alluvial deposits in mostly inactive alluvial-fans; typically sandy pebble- to cobble-sized gravel, and local boulders. Clasts are sub-rounded to sub-angular carbonate and quartzite derived from adjacent mountains. Surface morphology is generally planar with rounded margins. Incised drainages have a tributary pattern with channel incision ranging from 1–3 m. Soils consist of stage II–III $CaCO_3$ horizons (Bk) up to 1 m thick. Exposed thickness of the unit rarely exceeds 4 m. Qfi is faulted by the Independence Valley fault zone along the west side of the Pequop Mountains, with vertical separations up to 3 m.

Qlgo Older lacustrine gravels (late to middle Pleistocene?) Gray to brown deposits of moderately to well sorted pebble- to cobble-sized gravel and sand in an isolated beach bar remnant topographically above the late-Pleistocene shoreline gravels (Qlg). Clasts are rounded to subrounded. Soils consist of 1–1.5 m thick stage II–III $CaCO_3$ horizons (Bk). Unit was deposited by a pre-late Pleistocene lake in Independence Valley (Reheis, 1999). Exposed thickness of the unit does not exceed 3 m.

Qfo Older alluvial-fan deposits (middle Pleistocene?) Coarse-grained alluvial deposits in inactive alluvial fans; typically sandy pebble- to cobble-sized gravel with boulders. Clasts are subrounded to subangular carbonate and quartzite derived from the Pequop Mountains. Surface morphology ranges from planar to fully rounded erosional remnants. Locally mantled by an eolian cap. Surfaces without a significant eolian accumulation have abundant litter of pedogenic carbonate. Surfaces are highly dissected with incised channels up to 20 m deep. Upper soil horizons erosionally stripped, Stage III–IV $CaCO_3$ horizons up to 2.5 m thick form a continuous carbonate rich layer with local development of laminar carbonate structure. Qfo surfaces are commonly uplifted in the footwall of the Independence Valley fault zone. Late Quaternary displacement along the Independence Valley fault zone has uplifted Qfo surfaces approximately 30 m in the northern part of the map area, and 10–15 m to the south. An extensive Qfo surface near the outlet of Meyers canyon is topographically inset up to 12 m below a remnant of the QTf surface. Exposed thickness of the unit is 5 m to ~20 m.

QTb Boulder deposit in oldest alluvial-fan deposits (middle Pleistocene? to Pliocene?) Deposit consists of a lag of rounded to subangular boulders of Eureka Quartzite along a ~100 m wide belt that extends westward from Meyers canyon for ~1.2 km. Boulders are commonly as much as 4 to 5 m in greatest dimension and generally larger than 1 m in diameter. Any fine matrix has been eroded. Probably deposited as a coarse debris flow that was sourced from similarly coarse talus beneath cliffs of Eureka Quartzite in the northeastern part of the Meyers canyon drainage in the Pequop Summit quadrangle (Henry and Thorman, 2015) and flowed down the channel that drained Meyers canyon before capture by the current northwest-trending drainage. Approximately coeval with oldest alluvial-fan deposits (QTf).

QTf Oldest alluvial-fan deposits (middle Pleistocene? to Pliocene?) Coarse-grained alluvial deposits; typically sandy pebble- to cobble-sized gravel with boulders. Clasts are subrounded to subangular carbonate and quartzite derived from the Pequop Mountains. A morphologically rounded, eroded remnant of the QTf surface is preserved south of the outlet of Meyers canyon. Soils horizons are largely stripped; however, abundant litter of pedogenic carbonate suggest remnants of Stage IV–IV+ $CaCO_3$ horizons (Bk) of unknown thickness. QTf stratigraphically overlies Tg with a gradational and conformable contact. Exposed thickness of the unit ranges from 15 to ~25 m.

Tertiary Sedimentary Rocks

Tg Tertiary fanglomerate (Pliocene? to Miocene) Coarse gravel mostly expressed as a lag of boulders to pebbles of limestone, marble, and quartzite. Scattered outcrops show poorly bedded, poorly to moderately sorted, strongly to moderately calcite-cemented, fluvial gravel. Larger clasts are subangular to rounded, whereas smaller clasts are angular to subangular. Common imbrication of platy limestone and marble clasts indicates westward paleocurrents. Relative abundance of carbonate versus quartzite clasts varies north to south and probably reflects variable amount of quartzite exposure in drainages at the time, which seem to largely coincide with modern drainages. Discontinuous gravel lenses are interbedded near the top of the brown sandstone part of tuffaceous sediments (Ts), and gravel becomes predominant in the upper 10 m of the deposit. Maximum exposed unit thickness is 90 m. Younger than ca. 4.8 Ma, the weighted mean $^{40}Ar/^{39}Ar$ age of a group of the three youngest detrital sanidine grains (4.5, 5.2, and 5.7 Ma) out of 24 analyzed from an interbedded tephra (sample H17-32; table 1). Possibly younger than the ca. 4.5 Ma age of the youngest grain. Ages of other grains range from 10.3 to 1684 Ma.

Tls, (Oe), (Op), (Op*), (O€np) Tertiary landslide deposit (Miocene) Megabreccia landslide deposit exposed in the scarp and uplifted footwall of the Independence Valley fault zone. Individual large blocks, a minimum of about 8 m in diameter, commonly several tens of meters in diameter, and reaching 230 m long are mapped separately and identified by their primary rock type. Individual blocks are identified by continuity of bedding orientation over the entire block but are commonly brecciated at their margins. Rock types comprising individual blocks are Eureka Quartzite (Oe), undivided Pogonip Group (Op), Notch Peak Formation (O€np, distinguished by common dolomite and abundant, thin chert layers), and jasperoid (Op*, light red with preserved bedding, which suggests the rock is silicified Pogonip limestone) and undivided limestone, commonly showing small-scale internal folds. The individual blocks are the

Table 1. Summary of $^{40}Ar/^{39}Ar$ thermochronology results from the Pequop Mountains

Single crystal analyses on sanadine

Sample	Unit	Lat83	Long83	Age	±2σ	K/Ca	±1σ	*n*	Sample group	Comment
H17-32	Tg	40.99053	-114.63470	4.84	0.79	27.1	17.3	3/24	all data	Maximum age; youngest date = 4.46±0.24 Ma
H17-66	Ts	40.98078	-114.64449	6.23	0.02	39.4	9.3	3/23	high K/Ca group	All are reasonable
"	"			5.87	0.21	13.7	1.0	17/23	low K/Ca group	"
"	"			6.04	0.07	17.6	9.9	20/23	all data	"
H17-53	Ts	40.95686	-114.64283	10.31	0.03	54.2	6.2	6/24	all data	Best age estimate; one 8.14±0.03 Ma grain
WNC119-34	Ts	40.96452	-114.64935	9.84	0.11	11.7	5.6	5/24	sanidine	Best age estimate
"	"			10.14	0.09	0.20	0.01	11/24	plagioclase	Possible
"	"			9.85	0.07	3.8	6.2	16/24	all data	Possible
WNC119-425	Ts	40.96452	-114.64935	10.78	0.03	12.3	2.4	3/16	all data	2016 analysis
WNC119-425R	Ts	40.96452	-114.64935	10.74	0.03	14.2	2.2	3/24	all data	2018 analysis of new separate

Step heating analyses

Sample	Unit	Lat83	Long83	Material*	Integrated age	±2σ	"Plateau" range#	Comment
H18-648	Jl	40.965906	-114.53629	bt	136.3	0.70	140-130 Ma	
H15-35	Cd	40.936114	-114.62515	bt	78.0	0.10	ca. 80 Ma	
"	"	"	"	ms	78.0	0.07	ca. 75 Ma	
H18-627	Cd	41.003857	-114.61669	bt	87.7	0.09	ca. 90 Ma	
"	"	"	"	ms	76.7	0.30	80-70 Ma	
61418(2)	Cmp	40.974632	-114.60786	bt	77.8	0.07	ca. 80 Ma	
"	"	"	"	ms	78.6	0.05	ca. 80 Ma	
H17-23	Kg	40.942860	-114.62854	ms_MDD	74.3	0.03	ca. 70 Ma	
H18-23	Kg	40.930282	-114.64415	ms_MDD	67.9	0.03	70-65 Ma	MDD model for ms and kspar suggests Eocene reheating
"	"	"	"	kspar_MDD	41.90	0.01	ca. 40 Ma	
H18-24	CZpm	40.930476	-114.64437	ms_MDD	69.7	0.06	75-68 Ma	
H18-40	Kg	40.935810	-114.63277	ms_MDD	73.0	0.05	75-70 Ma	MDD model for ms and kspar suggests Eocene reheating
"	"	"	"	kspar_MDD	45.13	0.01	50-40 Ma	
H18-34	Jl	40.938972	-114.61790	ms	82.2	0.15	Cretaceous	Disturbed Cretaceous spectra

*Materals: biotite (bt), muscovite (ms) including MDD (ms_MDD), and alkali feldspar MDD (kspar_MDD); MDD is for multi-domain diffusion modeling (e.g., Lovera et al., 1989)

#visual approximation of spectrum's plateau

same units and have textural characteristics similar to rocks exposed along the western edge of the present Pequop Mountains, which allows them to be derived from there. Exposed thickness ranges from 20 m to 90 m. Age ca. 10 Ma based on age of surrounding tephra; see below.

Ts Tertiary tuffaceous sediments (Pliocene? to Miocene) Heterogeneous sequence of tuffaceous sandstone, siltstone, lesser conglomerate, and minor lacustrine limestone and pyroclastic-fall deposits. Two parts are recognizable in outcrop but insufficiently exposed to be mapped separately. Lower part is light-colored, variably calcite-cemented, shard-rich sandstone, siltstone, pebble conglomerate, and minor tuff. Sandstone is thick- to thin-bedded, and siltstone is platy bedded. Sandstone locally contains pumice up to 1 cm diameter. Upper part is light brown, massive to rarely thick- to medium-bedded, weakly calcite-cemented sandstone that contains sparse, matrix-supported clasts of quartzite, limestone, and marble to 15 cm. Irregularly bedded, white to cream-colored lacustrine limestone is locally exposed in both parts. The lower part commonly is expressed only as a nearly white soil, locally with mud cracks. The upper part is mostly covered by gravel eroding from overlying fanglomerate (Tg). Unit is up to approximately 350 m thick in the footwall of the Independence Valley fault zone. Unit Ts is interpreted to fill the late-Cenozoic depocenter in Independence Valley and may exceed 2 km thick in the deepest parts of the basin based on regional gravity modeling. New $^{40}Ar/^{39}Ar$ dates bracket the age of the deposit between approximately 6 Ma and > 10.8 Ma. The upper part of the brown sandstone is ca. 6.04±0.09 Ma, the weighted mean $^{40}Ar/^{39}Ar$ age of a homogeneous population of 20 of 23 analyzed sanidine grains from a tuff-rich bed (sample H17-66; table 1).

$^{40}Ar/^{39}Ar$ dates on three samples of the lower part range from ca. 9.9 to 10.8 Ma. Outcrop sample H17-53 yielded a weighted mean age of 10.31±0.03 Ma from a coherent group of 6 sanidine grains out of a total of 24 analyzed grains; older grains range from 10.36 to 38.88 Ma (table 1). Two samples from drillhole WNC119 yielded ages of 9.90±0.13 Ma (WNC119-34 foot depth; 5 sanidine grains out of 24, the rest of which are plagioclase) and 10.74±0.03 Ma (n = 3 of 24) and 10.78±0.03 Ma (n = 3 of 16) (WNC119-425 foot depth, separately prepared aliquots analyzed in 2018 and 2016) (table 1).

Eocene and Cretaceous(?) Intrusive Rocks

Tr Rhyolite dikes (Eocene) Northeast-striking, tan-weathering, sparsely porphyritic, and mostly non-resistant rhyolite sills and dikes intrude rocks of the Killian Springs Formation (Cks) and Toano Limestone (Ct) in the eastern part of the map area. Contacts and igneous foliations partly parallel host-rock foliations and partly crosscut them. Fewer than 1% phenocrysts of quartz and altered feldspar up to about 1 mm in diameter occur in a fine-grained matrix of quartz and feldspar with alteration products of sericite (muscovite?) or clay. In thin section, the matrix contains radial to irregular spheres that may be spherulites. Bedell et al. (2010) reported U-Pb zircon ages of 39.1±0.7 Ma and 41.0±0.8 Ma.

Kg Granitic sills and pods (Cretaceous) White leucogranite makes thin (0.5 to 3 m thick) sills and pods parallel to bedding in the Killian Springs Formation (Cks) and Toano Limestone (Ct). The fine- to coarse- grained leucogranite contains quartz, microcline, plagioclase, muscovite, and minor garnet. Based on a discordant age population of zircons, Bedell et al. (2010) concluded that the leucogranite is no older than Late Cretaceous. New $^{40}Ar/^{39}Ar$ step-heating of muscovite from several samples suggest that they are Late Cretaceous in age, cooling through muscovite closure temperatures at 70–85 Ma (Henry and Thorman, 2015; this study) (table 1; fig. 1). New multi-domain diffusion (MDD) modeling results from step-heated alkali feldspar $^{40}Ar/^{39}Ar$ analyses from the same samples as the muscovite analyses suggest a significant phase of Eocene reheating and subsequent cooling (table 1; fig. 1); MDD modeling not shown.

Paleozoic and Neoproterozoic Sedimentary Rocks

Paleozoic unit thicknesses are from this study, Thorman (1970), Camilleri (2010), Henry and Thorman (2015), and Zuza et al. (2018). Cambrian stratigraphy follows that of McCollum and Miller (1991). Due to internal folding within less competent units, probable bedding-plane faulting, boudinage development, attenuation faulting, and brecciation of competent units, thicknesses are best estimates where the rocks are undeformed or least deformed. Paleozoic rocks are exposed only along the eastern limit of the map area. Unit thickness varies significantly along strike and above and below the Independence thrust.

Pp Pequop Formation (Permian) Interbedded limestone, silty limestone, and dolomite, with Fusulinid-rich beds and irregular lenses of dark chert. The unit is not exposed in the map area, but was observed in borehole WNC119 where it structurally overlies Ordovician Fish Haven Dolomite. It is depicted in cross section A–A'–A". The Pequop Formation is exposed in the Independence Valley NE quadrangle to the east (Zuza et al., 2018) as part of a continuous stratigraphic section in the southeastern map area and in the Pequop structural plate in the northern map area, which is bounded by a low-angle normal fault. In the Pequop plate, at least 600 m of Pequop Formation is exposed, which probably correlates with the borehole observations in this map.

Ds Simonson Dolomite (Devonian) Lower part consists of laminated light-gray to black dolomite and minor gray-green laminated limestone. As many as three thin (0.5- to 2-m-thick) layers of light red-brown-weathering, planar to cross-bedded, siliceous to dolomitic quartzites are present at the base of the unit through much of the area. Upper part consists of interbedded dolomite and limestone, including Stringocephalus-bearing biostromes, and probably is equivalent to the Fox Mountain formation of Sandberg et al. (1997) and Sandberg and Morrow (2009). Ovoid to irregular boudins of dolomite up to 10 m long in foliated limestone are common. Thickness varies from 300 m to 400 m.

DSlm Lone Mountain Formation (Devonian to Silurian) Mostly light to very light gray, rarely medium gray, massive to faintly bedded dolomite. Approximately 150–180 m thick.

Srm Roberts Mountains Formation (Silurian) Thin-bedded to platy, fine-grained, medium to dark gray limestone and dolomite. Upper part more dolomitic; lower part more limestone. However, relative proportions of limestone and dolomite change gradationally along strike. Locally fossiliferous containing crinoid, brachiopod, and graptolite fragments. Approximately 140 m thick.

Sl Laketown Dolomite (Silurian) Interbedded light to medium gray, fine- to medium-grained dolomite. Lighter and darker intervals range from 15–30 m thick. Beds vary from massive, to fine to coarsely laminated, to mottled light-colored to grayish-black chert lenses are common. Bioclastic debris and well-preserved crinoids, corals, and brachiopods occur at several horizons. Contact with underlying Fish Haven Dolomite at base of lowest light gray dolomite. Approximately 85 m thick.

Ofh Fish Haven Dolomite (Upper Ordovician) Dark gray to black, massive to medium- to rarely thinly-bedded, fine-grained dolomite. Basal beds typically contain black to dark gray chert lenses. Bioclastic debris, especially of crinoids, is common. Rests conformably on the Eureka

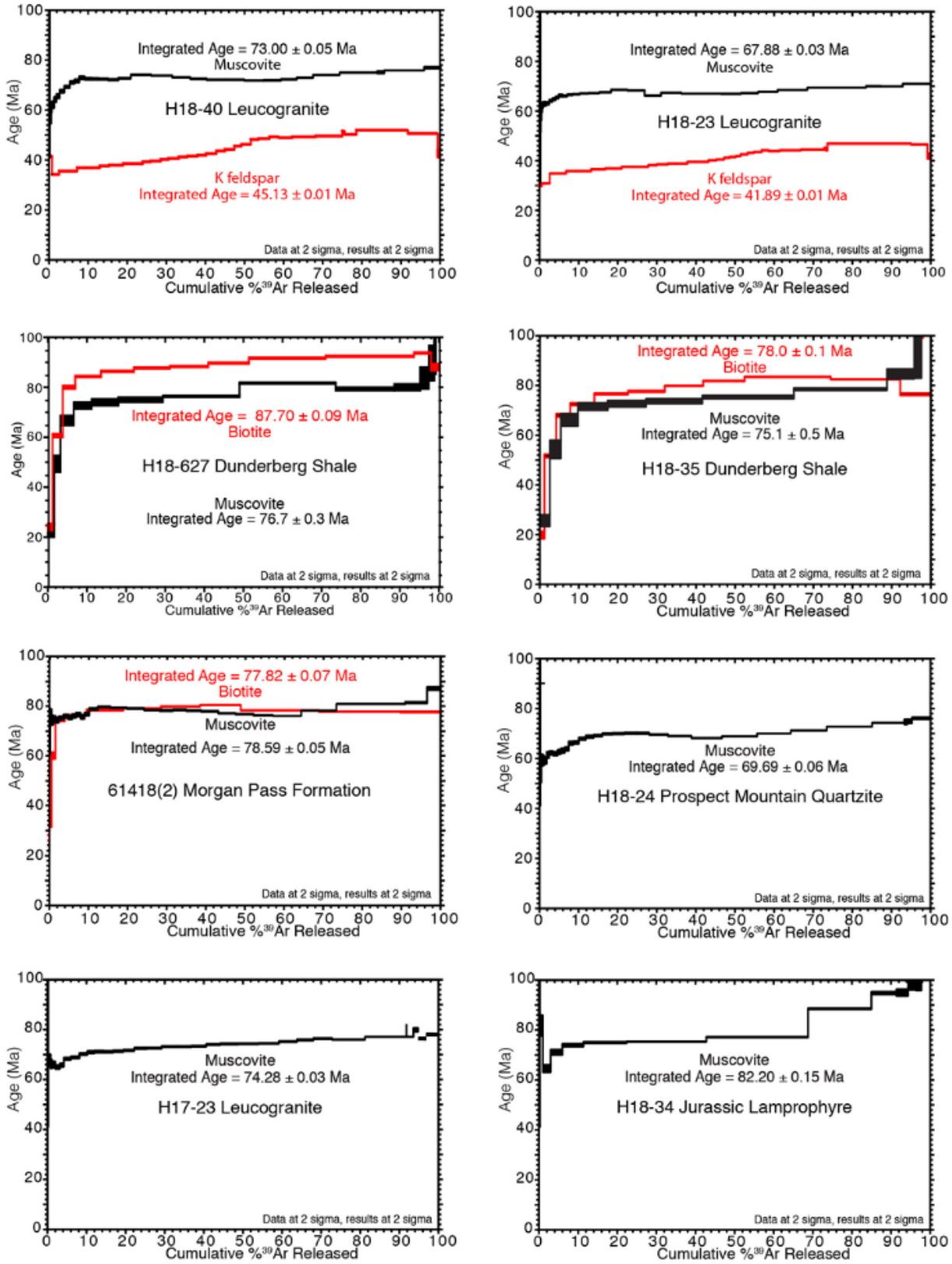

Figure 1. $^{40}Ar/^{39}Ar$ spectra for muscovite, K feldspar, and biotite of samples from the Pequop Mountains to determine the timing and rates of cooling and exhumation. All samples analyzed at the New Mexico Geochronological Research Laboratory, New Mexico Bureau of Geology and Mineral Resources in collaboration with Matthew Heizler. See text and tables 1 and 2 for further discussion.

Quartzite, but contact is commonly brecciated. Approximately 120–140 m thick.

Oe Eureka Quartzite (Middle Ordovician) Vitreous, mostly white to lesser medium gray to purple quartzite composed of medium-grained, rounded quartz grains that generally are frosted. The unit is generally intact in the map area, although it is variable brecciated in the Independence Valley NE quadrangle. The unit forms prominent light-colored cliffs of medium bedded, mostly planar to less commonly cross-bedded rock; cross beds typically expressed by light blue color bands where strongly silicified or by selective weathering of carbonate near base or top of formation. Basal and upper quartzite beds are generally darker than interior beds, ranging to medium to dark gray and purple. Thin sections from a sample collected from the prominent Oe cliff band on the western flank of the range shows quartz grains with shape-preferred orientations (SPO) but no lattice-preferred orientation (LPO). Quartz grain boundaries are comprised of small bulges and small recrystallized grains, suggesting bulging recrystallization. A slight polygonized texture and faint presence of subgrains suggests minor subgrain rotation recrystallization. Undulose extinction is common. These characteristics suggest that these rocks experienced temperatures of 300–400°C, which is corroborated Raman spectroscopy on carbonaceous material (RSCM), calcite-dolomite (CD), and conodont color alteration index (CAI) thermometry (Howland, 2016; Thorman et al., 2019; Zuza et al., 2019).

Pogonip Group The Pogonip Group, as mapped in this quadrangle, and the Independence Valley NE Pequop Summit quadrangles (Henry and Thorman, 2015; Zuza et al., 2018), includes the following formations:

Opl Lehman Formation (Lower Ordovician) Medium gray-blue, fine-grained platy to medium-bedded limestone with thin, tan, argillaceous interbeds and irregular bodies, possibly burrows. Locally contains abundant leperditia (small, pea-shaped ostracod). Grades upward into dark-gray dolomite (Crystal Peak Dolomite, not mapped separately here) and sandy dolomite of Eureka Quartzite. Approximately 150 m to 250 m thick.

Kanosh Formation The Kanosh Formation includes the following informal units: upper shale (Kanosh shale), middle limestone (Kanosh limestone), and basal quartzite (Kanosh quartzite).

Opks Kanosh shale (Lower Ordovician) Yellowish-brown, olive, gray to black, fissile shale with intercalated platy argillaceous limestone similar to Lehman Limestone. Forms covered slopes between bounding units and upper and lower contacts are covered. Limestone layers commonly contain abundant leperditia. Poorly exposed, but probably 20–30 m thick.

Opkl Kanosh limestone (Lower Ordovician) Limestone similar to Lehman Limestone. Approximately 160 m thick.

Opkq Kanosh quartzite (Lower Ordovician) Cross- to planar bedded, medium-grained, light brown to red-brown weathering, well-cemented quartzite with minor, commonly leached carbonate matrix. Locally absent between the House and Kanosh limestones, probably due to boudinage development. Etching of carbonate matrix due to weathering makes characteristic pitted surface and accentuates cross beds, which distinguishes it from Eureka Quartzite. Approximately 8 m thick.

Oph House Limestone (Lower Ordovician) Medium gray, fine-grained platy to medium-bedded limestone with argillaceous bedding planes and irregular bodies, possibly burrows. More shale and argillite component than Lehman Formation. Approximately 400 m thick.

O€np Notch Peak Formation (Lower Ordovician to Upper Cambrian) Predominantly light to medium gray dolomitic marble with local thick interbeds of blue and white limestone. Dolomitic marble is massive to banded light gray or tan to medium gray or tan. 2- to 5-cm-thick lenses and nodules of medium-gray chert are sparse to locally abundant, especially near the top of the formation. Limestone is well-bedded with tan, silty layers, similar to limestone of the Pogonip Group. Zebra dolomite makes a few beds in the upper part. Dolomite commonly forms ovoid to irregular boudins up to 10–15 m in diameter in flowed limestone. Contact with underlying Dunderberg Shale is gradational; dolomite or limestone are interbedded with phyllite and schist. No measured thickness in the map area, but Smith et al. (2013) show 380 m thickness and Camilleri (2010) suggest a range from 350 m to 600 m.

€d Dunderberg Shale (Cambrian) Recessive weathering, poorly exposed unit consisting of green and black shale metamorphosed to phyllite and schist, especially in the footwall of the Independence thrust, commonly with fine porphyoblasts. Numerous thin (≤10 cm) micaceous limestone interbeds. Muscovite is parallel to foliation and biotite is oblique to foliation. Two biotite-muscovite schist samples (H18-627 and H15-35) yielded muscovite and biotite $^{40}Ar/^{39}Ar$ cooling ages of 80–75 Ma and 90–80 Ma, respectively (table 1; fig. 1). The analyzed muscovite grains were significantly smaller than the biotite, which implies that the effective Ar closure temperature in muscovite could have been equal or lower than that of biotite. The simplest interpretation is that both phases record protracted cooling through 350–300°C during the 75–90 Ma Late Cretaceous range, with sample variability reflecting variable Ar retention due to grain-size and other variabilities. The oblique biotite probably grew during a Late Cretaceous thermal pulse, cross cutting preexisting muscovite foliation, and both phases record cooling following this event. Sharp contact with underlying Oasis Formation. Approximately 50–60 m thick in the map area.

€o Oasis Formation (Cambrian) Cliff-forming white, light gray, and blue-gray medium- to thick-bedded

limestone and dolomite marble. White and light gray limestone and dolomite make up the top and bottom of the unit, and blue-gray limestones, similar in appearance to Clifside Limestone, make up the middle of the formation. Tan silt beds appear similar to those in Pogonip limestones but are commonly more sheared. The occurrence of thin-bedded silty limestone or shale marks the contacts with overlying and underlying Dunderburg and Shafter, respectively. Approximately 200 m thick.

Ꞓs Shafter Formation (Cambrian) Thinly bedded gray to blue limestone marble with silty orange to gray interbeds commonly metamorphosed to phyllite or schist. Unit is recessive, with areas weathered to dark brown. Approximately 130 m thick in the map area.

Ꞓdl Decoy Limestone (Cambrian) Distinctive cliff-forming tan-gray recrystallized dolomite or light blue-gray recrystallized limestone with silty limestone interbeds. Can resemble Clifside Limestone where not dolomitized or deformed. Contact with underlying recessive Morgan Pass Formation occurs with the appearance of silty limestone. Variably 30 m to 60 m thick.

Ꞓmp Morgan Pass Formation (Cambrian) Recessive weathering shale and platy blue limestone. Metamorphosed to micaceous schist and marble. Muscovite is parallel to foliation and biotite, where observed, is oblique to foliation. A biotite-muscovite schist sample (61418(2)) yielded similar muscovite and biotite $^{40}Ar/^{39}Ar$ cooling ages of ~80 Ma (table 1; fig. 1). The analyzed muscovite grains were significantly smaller than the biotite, which implies that the effective Ar closure temperatures of the two phases may have been comparable. The oblique biotite probably grew during a Late Cretaceous thermal pulse, cross cutting preexisting muscovite foliation, and both phases record cooling of this event. The contact with the underlying Clifside is sharp at the base of the lowest shale or silty limestone above the distinct cliff-forming gray Clifside Limestone. Approximately 120 m thick in the map area.

Ꞓcl Clifside Limestone (Cambrian) Wavy-foliated, light gray-blue calcareous marble, commonly with coarse muscovite, with gray or orange-brown silty layers and locally, abundant crinoids and other strongly recrystallized fossils. A minor brown silty limestone section, metamorphosed to muscovite-biotite schist, near the middle of the Clifside is recessive and poorly exposed. Thickness varies substantially in the map area, from 100 m to 200 m.

Ꞓt Toano Limestone (Cambrian) Foliated, dark grayish green micaceous marble with much less phyllite and tremolite schist than in underlying Killian Springs Formation. Protoliths were likely thin-bedded limestone and silty limestone. Some beds are chaotically folded, probably due to slumping and soft-sediment deformation because the enveloping layers are not deformed. The contact with the overlying Clifside Limestone is placed at the distinct color and lithologic change, Toano being darker green and more micaceous. Approximately 170 m thick in the map area.

Ꞓks Killian Springs Formation (Cambrian) Black to dark greenish gray micaceous marble, phyllite, and biotite-muscovite or hornblende schist with tremolite-bearing layers. Protoliths were likely siltstone, calcareous siltstone and thin-bedded limestone. Contact with underlying Cambrian Prospect Mountain Quartzite is sharp. Approximately 170 m thick in the map area.

ꞒZpm Prospect Mountain Quartzite (Lower Cambrian to Neoproterozoic) Light to blue gray massive quartzite with minor, cm-thin, garnet-bearing micaceous layers. Fine to medium grained with quartz-pebble conglomerate layers. Planar to cross-bedded. In thin section, quartz grains exhibit a strong SPO, but weak LPO. Highly lobate interfingering quartz grain boundaries suggest that grain boundary migration recrystallization of the quartz at temperatures >500°C. Peak temperatures of 500–600°C affecting the Prospect Mountain Quartzite are corroborated by the presence of garnet and RSCM thermometry (Howland, 2016; Zuza et al., 2019). New $^{40}Ar/^{39}Ar$ step-heating of muscovite (sample H18-24) from this unit suggests Late Cretaceous 75–68 Ma cooling through muscovite closure temperatures (table 1; fig. 1).

Zmc McCoy Creek Group (Neoproterozoic) This unit is not exposed in the map area, but is stratigraphically below Prospect Mountain Quartzite and is depicted on the cross sections. Comprised of quartzite, conglomerate, and argillite with minor limestone. Thickness probably exceeds 1500 m as observed in the Pilot Range to the east (Miller and Lush, 1981).

ACKNOWLEDGMENTS

We greatly thank Tom Anderson, Steve Ruppel, and Fred Zoerner for considerable help in recognizing and interpreting stratigraphic, sedimentologic, and structural characteristics of the rocks of the Pequop Mountains. This map benefitted from helpful discussions with Gregg Loptien and Chrissy Ricks at Agnico Eagle Mined and Jeff Blackmon at Newmont Mining Corporation. We also greatly thank Matt Heizler and Bill McIntosh of the New Mexico Geochronological Research Laboratory for guidance in their exceptional $^{40}Ar/^{39}Ar$ lab. Research supported by the U.S. Geological Survey, National Cooperative Geologic Mapping Program, under USGS award number G18AC00198 (2019) and G16AC00186 (2017). The views and conclusions contained in this document are those of the authors and should not be interpreted as necessarily representing the official policies, either expressed or implied, of the U.S. Government.

REFERENCES

Bedell, R., Struhsacker, E., Craig, L., Miller, M., Coolbaugh, M., Smith, J., and Parratt, R., 2010, The Pequop mining district, Elko County, Nevada—an evolving new gold district: Society of Economic Geologists, Special Publication Number 15, p. 29–56.

Camilleri, P.A., 2010, Geologic map of the northern Pequop Mountains, Elko County, Nevada: Nevada Bureau of Mines and Geology Map 171, scale 1:48,000, 15 p.

Henry, C.D., and Thorman, C.H., 2015, Preliminary geologic map of the Pequop Summit quadrangle, Elko County, Nevada: Nevada Bureau of Mines and Geology Open-File Report 15-8, scale 1:24,000, 12 p.

Howland, C., 2016, High thermal gradient in the upper plate of a core complex, determined by calcite-dolomite and RSCM thermometry, Pequop Mountains, NV [BS Honors Thesis]: Union College, 135 p.

Kuiper, K.F., Deino, A., Hilgen, F.J., Krijgsman, W., Renne, P.R., and Wijbrans, A.J., 2008, Synchronizing rock clocks of Earth history: Science, v. 320, no. 5875, p. 500–504.

Lovera, O.M., Richter, F.M., and Harrison, T.M., 1989, The $^{40}Ar/^{39}Ar$ thermochronometry for slowly cooled samples having a distribution of diffusion domain sizes: Journal of Geophysical Research: Solid Earth, v. 94, no. B12, p. 17917–17935.

McCollum, L.B., and Miller, D.M., 1991, Cambrian stratigraphy of the Wendover area, Utah and Nevada: U.S. Geological Survey Bulletin 1948, 43 p.

Miller, D. M., and Lush, A. P., 1981, Preliminary geologic map of the Pilot Peak and adjacent quadrangles, Elko County, Nevada, and Box Elder County, Utah: U.S. Geological Survey Open-File Report 81-658.

Min, K., Mundil, R., Renne, P. R., and Ludwig, K. R., 2000, A test for systematic errors in $^{40}Ar/^{39}Ar$ geochronology through comparison with U/Pb analysis of a 1.1-Ga rhyolite: Geochimica et Cosmochimica Acta, v. 64, no. 1, p. 73–98.

Munroe, J.S., and Laabs, B.J.C., 2013, Temporal correspondence between pluvial lake highstands in the southwestern U.S. and Heinrich Event 1. J. Quaternary Science, 28, p. 49–58.

Reheis, M.C., 1999, Extent of Pleistocene lakes in the western Great Basin: Reston, Virginia, USA: U.S. Geological Survey Miscellaneous Field Studies MF-2323.

Sandberg, C.A., and Morrow, J.R., 2009, Recognition of Fox Mountain Formation solves enigmatic Devonian stratigraphy in central and northern Utah: Geological Society of America Abstracts with Programs, v. 41, no. 6, p. 15.

Sandberg, C.A., Morrow, J.R., and Warme, J.E., 1997, Late Devonian Alamo impact event, global Kellwasser events, and major eustatic events, eastern Great Basin, Nevada and Utah: Brigham Young University Geology Studies, v. 41, p. 129–160.

Smith, M.T., Rhys, D., Ross, K., Lee, C., and Gray, J.N., 2013, The Long Canyon deposit—anatomy of a new off-trend sedimentary rock-hosted gold discovery in northeastern Nevada: Economic Geology, v. 108, p. 119–145.

Steiger, R., and Jäger, E., 1977, Subcommission on geochronology—convention on the use of decay constants in geo-and cosmochronology: Earth and Planetary Science Letters, v. 36, no. 3, p. 359–362.

Taylor, J.R., 1982. An introduction to error analysis—the study of uncertainties in physical measurements: University Science Books, Mill Valley, California, 270 p.

Thorman, C.H., 1970, Metamorphosed and nonmetamorphosed Paleozoic rocks in the Wood Hills and Pequop Mountains, northeast Nevada: Geological Society of America Bulletin, v. 81, p. 2417–2448.

Thorman, C.H., Sandberg, C.A., Henry, C.D., Zuza, A.V., and Ressel, M.W., 2019, Regional tectonics and conodont CAIs indicate normal burial depths, not Mesozoic thickening, in the Pequop Mountains, NE Nevada: Geological Society of America Abstracts with Programs. Vol. 51, No. 4.

Zuza, A.V., Henry, C.D., Ressel, M.W., Thorman, C.H., Dee, S., and Blackmon, J.E., 2018, Preliminary geologic map of the Independence Valley NE quadrangle, Elko County, Nevada: Nevada Bureau of Mines and Geology Open-File Report 18-4, scale 1:24,000, 12 p.

Zuza, A.V., Henry, C.D., Ressel, M.W., Thorman, C.H., Dee, S., Long, S.P., 2019, Probing the core of the North American Cordillera—insights from geologic mapping of the Pequop Mountains, NE Nevada: Geological Society of America Abstracts with Program, v. 51, no. 4.

Suggested Citation:

Zuza, A.V., Dee, S., Henry, C.D., Ressel, M.W., and Thorman, C.H., 2019, Geologic map of the Independence Valley NW quadrangle, Elko County, Nevada: Nevada Bureau of Mines and Geology Open-File Report 19-3, scale 1:24,000, 18 p.

© Copyright 2019 The University of Nevada, Reno. All Rights Reserved.

Table 2. $^{40}Ar/^{39}Ar$ analytical data for single crystal analyses

Sample: H17-32
Material: Sanidine

	N	Tag	Age (Ma)	±1σ (Ma)	K/Ca	±1σ	K/Cl	±1σ	%^{40}Ar	$^{40}Ar^{*}/^{39}Ar_{K}$
X	01	omit	25.37	0.01	35.30	0.62	171900.22	475855.93	99.35	3.58
X	02	omit	26.64	0.03	66.06	5.06	864.98	27.38	95.57	3.77
	03	ok	5.18	0.87	0.00	0.00	100.43	17.97	40.26	0.73
X	04	omit	10.28	0.33	49.81	55.51	1755.73	1973.36	82.52	1.45
X	05	omit	14.72	0.19	18.79	4.13	3071.74	3006.23	90.95	2.07
X	06	invalid	697.57	239.61	0.00	0.00	15.49	9.61	47.28	119.14
X	07	invalid	140.54	476.51	0.00	0.00	-2.85	9.82	2.27	20.50
X	08	invalid	108.73	49.78	0.71	0.37	16.47	7.95	1.08	15.72
X	09	invalid	63.11	1586.86	0.04	0.92	-0.69	16.09	0.29	9.01
X	10	invalid	0.00	0.00	-0.20	1.15	-0.81	4.35	95.52	-13446.19
X	11	omit	33.49	0.13	28.81	4.79	-10412.59	19591.14	95.42	4.74
X	12	invalid	288.28	34.30	0.51	0.09	7.03	1.02	56.23	43.81
X	13	omit	25.42	0.03	31.70	1.44	16653.66	12306.42	98.93	3.59
	14	ok	4.46	0.24	39.29	24.34	1524.94	1012.75	67.57	0.63
X	15	omit	25.22	0.03	54.87	4.90	-17289.10	14667.53	97.45	3.56
X	16	invalid	1684.38	189.37	2.45	2.16	19.70	5.70	94.93	387.78
X	17	omit	20.48	0.06	151.89	77.88	7107.02	5321.73	97.90	2.89
	18	ok	5.72	0.39	14.85	5.34	151.30	16.85	59.11	0.80
X	19	omit	18.72	0.21	11.53	1.50	128.38	5.89	90.56	2.64
X	20	invalid	948.55	1533.16	0.00	0.00	1.74	3.65	71.87	174.39
X	21	invalid	104.13	30.75	0.00	0.00	69.94	104.69	31.21	15.03
X	22	omit	40.50	0.06	317.35	241.92	5822.93	2652.87	96.29	5.75
X	23	invalid	1152.00	635.93	0.00	0.00	27.33	45.62	63.94	225.09
X	24	omit	25.06	0.14	23.39	4.11	3093.83	2474.09	95.77	3.54
Weighted mean Age ±2σ			**4.84**	**0.79**	**n=3/24**	**MSWD=*3.915**				
Isochron Age ±2σ			**3.85**	**1.78**		**MSWD=2.431**				

Sample: H17-53
Material: Sanidine

	N	Tag	Age (Ma)	±1σ (Ma)	K/Ca	±1σ	K/Cl	±1σ	%^{40}Ar	$^{40}Ar^{*}/^{39}Ar_{K}$
	01	ok	10.32	0.01	57.81	2.20	-51170.61	65907.63	98.05	1.45
X	02	omit	33.50	0.02	116.01	11.47	43116.43	54799.43	98.33	4.74
	03	ok	10.31	0.01	46.95	1.57	-26164.96	15293.12	98.79	1.45
X	04	omit	14.14	0.03	20.53	0.76	3371.24	719.71	96.25	1.99
X	05	omit	25.75	0.02	78.06	6.03	-63903.58	142911.08	96.55	3.64
X	06	omit	29.57	0.03	77.92	8.37	68725.28	238654.33	99.25	4.18
	07	ok	10.31	0.01	57.77	2.36	-23819.04	14450.17	98.31	1.45
X	08	omit	10.37	0.06	55.77	11.42	-1093674.33	137887283.61	96.24	1.46
X	09	omit	8.14	0.03	52.91	7.60	-31065.42	88716.84	98.16	1.14
X	10	omit	22.91	0.03	67.65	6.52	25044.20	32319.86	97.93	3.23
X	11	omit	25.02	0.03	54.72	4.43	43571.63	97202.93	97.92	3.53
X	12	omit	10.55	0.02	67.78	7.54	18685.64	20858.10	98.28	1.48
X	13	omit	35.33	0.03	104.01	13.03	27184.31	33647.26	99.41	5.00
X	14	omit	34.97	0.22	107.75	119.08	3343.87	4229.59	93.99	4.95
X	15	omit	10.37	0.03	49.35	4.61	29761.28	42795.79	97.67	1.46
	16	ok	10.31	0.04	56.37	7.91	5841.07	2559.46	96.33	1.45
X	17	omit	10.36	0.02	43.46	2.24	-13258.58	6359.51	97.26	1.46
	18	ok	10.31	0.03	60.30	5.62	-29106.38	44874.81	96.67	1.45

Sample: H17-53, Material: Sanidine (continued)

	N	Tag	Age (Ma)	±1σ (Ma)	K/Ca	±1σ	K/Cl	±1σ	%^{40}Ar	^{40}Ar*/^{39}Ar$_K$
X	19	omit	25.46	0.04	46.47	4.04	-16055.50	17246.45	97.43	3.60
X	20	omit	27.51	0.03	817.48	533.12	16953.21	8823.08	91.53	3.89
	21	ok	10.32	0.02	45.75	2.97	38847.23	64094.93	97.98	1.45
X	22	omit	13.90	0.04	20.61	1.53	11177.53	15712.56	97.79	1.96
X	23	omit	38.88	0.24	32.52	12.32	-2660.63	2567.41	98.80	5.51
X	24	omit	22.46	0.03	220.80	67.58	7536.50	2750.51	95.84	3.17
Weighted mean Age ±2σ			**10.31**	**0.03**	**n=6/24**	**MSWD=*0.064**				
Isochron Age ±2σ			**10.31**	**0.03**		**MSWD=*0.080**				

Sample: H17-66
Material: Sanidine

	N	Tag	Age (Ma)	±1σ (Ma)	K/Ca	±1σ	K/Cl	±1σ	%^{40}Ar	^{40}Ar*/^{39}Ar$_K$
X	01	omit	6.51	0.05	63.07	13.10	-2733.11	780.34	95.95	0.91
X	02	omit	6.66	1.46	0.00	0.00	-192.40	109.34	51.96	0.94
	03	ok	6.13	0.08	13.62	0.89	108.83	1.92	92.72	0.86
X	04	omit	25.43	0.03	13.64	0.29	26530.22	39532.52	99.38	3.59
	05	ok	6.16	0.06	41.65	8.03	-5264271.38	3276873714.09	94.89	0.86
	06	ok	5.99	0.07	14.28	0.84	120.07	2.08	93.45	0.84
	07	ok	6.11	0.03	47.39	4.61	14124.20	9884.53	96.75	0.86
	08	ok	6.28	0.09	14.22	1.13	107.77	2.05	91.76	0.88
	09	ok	5.88	0.10	12.07	0.77	111.91	2.70	88.92	0.83
	10	ok	5.72	0.10	13.82	1.07	115.29	2.41	85.85	0.80
	11	ok	6.19	0.12	12.00	0.97	101.96	2.68	86.94	0.87
	12	ok	5.87	0.09	13.94	0.87	116.17	2.19	89.51	0.82
	13	ok	5.76	0.08	15.62	0.90	120.77	2.43	89.14	0.81
	14	ok	5.82	0.11	13.43	0.93	105.95	2.30	86.23	0.82
	15	ok	5.95	0.08	14.61	0.91	114.64	2.14	91.54	0.83
	16	ok	6.05	0.08	12.80	0.64	109.27	1.97	92.67	0.85
	17	ok	5.66	0.09	15.52	0.91	128.55	3.33	89.23	0.79
	18	ok	5.82	0.10	12.99	0.88	106.39	2.95	86.39	0.82
	19	ok	5.79	0.10	13.27	0.72	110.34	3.31	87.16	0.81
	20	ok	5.47	0.23	14.59	2.31	115.82	4.93	77.63	0.77
	21	ok	5.88	0.16	13.02	1.35	107.07	3.91	84.57	0.83
	22	ok	6.14	0.03	29.24	1.57	89444.42	510969.99	95.35	0.86
	23	ok	5.57	0.13	13.39	0.97	113.58	3.50	84.26	0.78
Weighted mean Age ±2σ			**6.04**	**0.07**	**n=20/23**	**MSWD=*6.089**				
Isochron Age ±2σ			**6.15**	**0.09**		**MSWD=*5.209**				

Sample: WNC119-34
Material: Sanidine

	N	Tag	Age (Ma)	±1σ (Ma)	K/Ca	±1σ	K/Cl	±1σ	%^{40}Ar	^{40}Ar*/^{39}Ar$_K$
X	01	**omit**	10.07	0.04	0.20	0.00	3266.39	580.37	95.72	1.41
X	02	omit	16.81	0.20	0.16	0.00	3817.92	3775.65	72.85	2.37
X	03	**omit**	10.63	0.38	0.20	0.00	1493.59	1467.22	80.50	1.49
X	04	omit	7.45	0.11	0.73	0.00	172.86	7.36	89.19	1.05
	05	ok	9.96	0.01	17.45	0.23	33474.41	31457.88	98.90	1.40
	06	ok	9.97	0.04	2.68	0.02	85027.69	547256.69	96.71	1.40
X	07	**omit**	10.61	0.19	0.18	0.00	-1384.44	725.40	88.71	1.49
	08	ok	9.69	0.33	0.19	0.00	-2267.28	3329.70	73.41	1.36
X	09	omit	11.15	0.47	0.17	0.00	-6093.02	30816.16	83.50	1.57
X	10	**omit**	10.07	0.15	0.18	0.00	10154.64	30036.91	91.19	1.41

Sample: WNC119-34, Material: Sanidine, (continued)

	N	Tag	Age (Ma)	±1σ (Ma)	K/Ca	±1σ	K/Cl	±1σ	%^{40}Ar	^{40}Ar*/^{39}Ar$_K$
X	11	**omit**	10.13	0.08	0.20	0.00	4579.00	2808.50	95.49	1.42
	12	ok	9.68	0.01	11.00	0.06	1551.36	49.47	98.50	1.36
	13	ok	9.90	0.01	14.76	0.09	-39824.85	29792.81	98.81	1.39
X	14	omit	11.21	0.32	0.16	0.00	1092.19	568.61	69.75	1.58
X	15	**omit**	10.40	0.09	0.21	0.00	6133.32	5582.84	95.26	1.46
X	16	omit	13.19	0.15	0.18	0.00	5657.05	7714.69	89.14	1.85
X	17	omit	12.14	0.11	0.17	0.00	1959.79	789.59	88.73	1.71
	18	ok	9.99	0.06	12.14	0.66	26050.96	82810.52	94.55	1.40
X	19	omit	13.68	0.06	14.34	0.49	442.26	21.75	86.66	1.92
X	20	**omit**	10.10	0.15	0.21	0.00	2096.58	1087.80	90.96	1.42
X	21	**omit**	10.47	0.20	0.22	0.00	2889.26	2900.44	95.05	1.47
	22	**ok**	9.98	0.35	0.19	0.00	-1846.19	2402.50	79.18	1.40
X	23	omit	13.53	0.14	0.19	0.00	3617.25	3025.11	86.34	1.90
X	24	**omit**	10.32	0.28	0.20	0.00	1595.88	1264.15	83.98	1.45
Weighted mean Age ±2σ			**9.84**	**0.09**	**n=7/24**	**MSWD=*58.009**				
Isochron Age ±2σ			**9.97**	**0.25**		**MSWD=*35.426**				

Sample: WNC119-425
Material: Sanidine

	N	Tag	Age (Ma)	±1σ (Ma)	K/Ca	±1σ	K/Cl	±1σ	%^{40}Ar	^{40}Ar*/^{39}Ar$_K$
X	01	omit	13.24	0.03	18.20	0.42	446.86	8.40	87.34	1.86
X	02	invalid	274.27	748.94	0.00	0.00	4.02	12.32	-18.40	41.41
X	03	invalid	-15.00	5.06	0.00	0.00	27.37	11.13	-83.91	-2.09
X	04	invalid	-36.19	18.65	0.10	0.04	1.02	0.41	-17.29	-5.02
X	05	omit	11.13	0.01	13.28	0.03	12900.86	1942.36	81.15	1.56
X	06	omit	77.50	0.31	193.98	382.42	902.08	229.19	92.99	11.08
X	07	omit	33.39	0.07	73.89	19.40	6878.10	4875.28	97.37	4.71
X	08	invalid	9.12	5.12	1.33	0.76	300.53	1256.83	11.94	1.28
X	09	invalid	-4760.94	96973.39	9.45	719.26	2.80	12.09	-0.57	-237.11
X	10	omit	15.31	0.01	9.45	0.02	13590.94	1921.76	99.30	2.15
X	11	omit	14.86	0.01	16.84	0.17	92806.35	174373.14	99.18	2.09
	12	ok	10.74	0.01	13.54	0.07	35766.10	21698.11	98.69	1.51
X	13	omit	14.57	0.01	19.32	0.10	-2737590.33	93033478.21	99.09	2.05
X	14	invalid	-98.02	90.35	0.00	0.00	-45.09	128.78	-52.67	-13.36
X	15	invalid	-14.25	7.02	0.96	0.53	31.38	21.37	-36.50	-1.99
X	16	omit	12.45	0.03	68.29	8.60	24871.14	36165.06	97.09	1.75
X	17	omit	13.19	0.02	20.94	0.52	-44242.37	73297.75	98.82	1.85
	18	ok	10.73	0.01	12.43	0.07	20873.85	6952.81	97.90	1.51
X	19	omit	11.59	0.01	21.72	0.11	63359.56	50006.64	99.25	1.63
X	20	omit	13.22	0.01	19.62	0.26	83606.61	148357.41	98.89	1.86
X	21	invalid	-36.40	13.71	0.71	0.39	128.19	395.13	-89.95	-5.04
X	22	omit	12.44	0.03	14.75	0.22	15126.25	6804.76	86.37	1.75
X	23	omit	14.31	0.02	21.59	0.40	131137.55	419519.05	99.00	2.01
	24	ok	10.73	0.01	16.61	0.17	101569.50	234558.88	97.57	1.51
Weighted mean Age ±2σ			**10.74**	**0.03**	**n=3/24**	**MSWD=0.096**				
Isochron Age ±2σ			**10.74**	**0.03**		**MSWD=0.009**				

Notes:

Isotopic ratios corrected for blank, radioactive decay, and mass discrimination, not corrected for interfering reactions.

X symbol preceding sample ID denotes analyses excluded from weighted-mean age calculations.

Notes and abbreviations: n/nt = number of analyses use to compute age/total analyses, MSWD = Mean Square of Weighted Deviates.

Sample preparation: Minerals were separated by crushing and sieving, followed by etching in 7% HF (sanidine only) or 7% HCl and rinsing in an ultrasonic bath, then concentrated using a Franz magnetic separator and/or density liquids, followed by hand picking.

Irradiation: Samples and Fish Canyon Tuff sanidine monitors in machined aluminum trays were irradiated *in-vacuo* at the Denver USGS Triga reactor.

Instrumentation and procedures: Samples heated using a defocused CO_2 laser for 30 seconds. Reactive gases removed during analysis by reaction with a SAES NP-10 getter. Analyses were performed using Thermo Argus VI and/or Helix mass spectrometers on line with automated all-metal extraction system.

J-factors were determined by CO_2 laser-fusion of 4 to 6 single crystals from multiple radial positions around the irradiation tray.

Age and error calculations: Mean age errors quoted as ±2σ, all other errors ±1σ. Calculations performed using Pychron software. Weighted-mean and error are inverse-variance-weighted mean and error Taylor (1982), with error multiplied by root MSWD where MSWD>1.

Constants: Decay constants after Min et al. (2000), λK_{total} = 5.464e-10/a. Isotopic abundances after Steiger and Jäger (1977). Ages calculated relative to FC-2 Fish Canyon Tuff sanidine interlaboratory standard at 28.201 Ma after Kuiper et al.(2008).

Table 3. $^{40}Ar/^{39}Ar$ analytical data for step heated analyses

ID	Power (Watts)	$^{40}Ar/^{39}Ar$	$^{37}Ar/^{39}Ar$	$^{36}Ar/^{39}Ar$ (x 10^{-3})	$^{39}Ar_K$ (x 10^{-15} mol)	K/Ca	$^{40}Ar^*$ (%)	^{39}Ar (%)	Age (Ma)	±1s (Ma)
H18-627, Biotite, 1.43 mg, J=0.0015578±0.04%, D=1±0, NM-303D, Lab#=66836-01										
Cambrian Dunderberg Shale, biotite-muscovite schist (N41.003857; W114.61669)										
A	0.5	35.09	0.0203	90.55	3131.2	25.2	23.7	1.3	23.60	0.59
B	0.8	29.67	0.0510	27.34	6373.1	10.0	72.8	3.9	60.55	0.34
C	1.0	33.01	0.0310	14.92	8009.3	16.5	86.7	7.2	79.80	0.31
D	1.5	33.73	0.0375	12.30	15670.6	13.6	89.2	13.6	83.88	0.17
E	2.0	34.19	0.0244	11.16	20786.5	20.9	90.4	22.2	86.03	0.14
F	2.5	34.34	0.0238	10.32	22055.3	21.5	91.1	31.2	87.12	0.14
G	3.0	34.51	0.0130	9.999	23892.4	39.3	91.4	41.0	87.85	0.13
H	3.5	34.67	0.0106	8.243	25623.4	48.3	93.0	51.6	89.68	0.12
I	5.0	34.77	0.0277	6.462	47420.2	18.4	94.5	71.0	91.40	0.07
J	7.0	35.88	0.0207	9.203	55200.7	24.7	92.4	93.7	92.21	0.07
K	9.0	35.69	0.0246	7.194	10781.2	20.7	94.0	98.1	93.29	0.27
L	15.0	34.34	0.0765	9.671	4559.2	6.7	91.7	100.0	87.66	0.55
Integrated age ± 2s			n=12			21.0			87.70	0.11
Isochron±2s		steps A-L	n=12	MSWD=404.68		$^{40}Ar/^{36}Ar$=	-82.8±2.5		99.30	0.19
61418(2), Biotite, 1.3 mg, J=0.0015594±0.04%, D=1±0, NM-303D, Lab#=66837-01										
Cambrian Morgan Pass Formation, biotite-muscovite schist (N40.974632; W114.60786)										
A	0.5	61.00	0.1396	165.4	988.2	3.7	19.9	0.4	34.31	1.65
B	0.8	26.78	0.2916	18.54	2619.7	1.7	79.6	1.6	59.90	0.71
C	1.0	29.43	0.1461	9.479	5017.8	3.5	90.5	3.8	74.51	0.43
D	1.5	29.57	0.1601	7.967	12923.5	3.2	92.1	9.5	76.14	0.18
E	2.0	29.41	0.1897	4.858	21226.8	2.7	95.2	18.9	78.22	0.11
F	2.5	29.25	0.2061	3.487	21667.4	2.5	96.5	28.5	78.89	0.11
G	3.0	29.47	0.0323	3.153	22648.7	15.8	96.8	38.6	79.70	0.10
H	3.5	29.63	0.0093	3.009	23297.1	54.9	97.0	48.9	80.27	0.11
I	5.0	28.47	0.0019	1.623	45141.5	266.6	98.3	68.9	78.19	0.06
J	7.0	28.09	0.0054	1.161	46791.3	93.7	98.8	89.6	77.55	0.05
K	15.0	28.10	0.0579	1.242	23410.2	8.8	98.7	100.0	77.51	0.10
Integrated age ± 2s			n=11			7.8			77.82	0.10
Isochron±2s		steps A-K	n=11	MSWD=172.05		$^{40}Ar/^{36}Ar$=	235.0±7.0		78.57	0.10

H15-35, Biotite, 1.31 mg, J=0.0015393±0.02%, D=1±0, NM-303C, Lab#=66835-01

Cambrian Dunderberg Shale, biotite-muscovite schist (40.936114; W114.62515)

A	0.5	39.16	-0.0318	108.8	0.5	-	17.9	1.2	19.69	0.75
B	0.8	32.38	0.0420	46.74	1.3	12.1	57.3	4.4	51.59	0.36
C	1.0	33.14	0.0464	29.01	1.4	11.0	74.1	7.9	67.97	0.32
D	1.5	33.07	0.0303	23.41	2.6	16.9	79.1	14.0	72.26	0.21
E	2.0	33.62	0.0271	20.09	3.6	18.8	82.3	22.7	76.38	0.16
F	2.5	34.34	0.0246	21.21	3.9	20.7	81.8	32.1	77.44	0.16
G	3.0	33.86	0.0225	16.74	4.1	22.7	85.4	42.0	79.71	0.14
H	3.5	33.60	0.0123	13.35	4.4	41.5	88.3	52.6	81.70	0.14
I	5.0	33.42	0.0133	10.64	9.1	38.2	90.6	74.6	83.38	0.08
J	7.0	33.42	0.0268	11.89	7.3	19.0	89.5	92.3	82.39	0.09
K	15.0	33.76	0.0385	20.62	3.2	13.3	82.0	100.0	76.35	0.18
Integrated age ± 2s			n=11		41.4	21.9			77.96	0.10
Isochron±2s		steps A-K	n=11	MSWD=61.20		$^{40}Ar/^{36}Ar=$	23.3±1.8		91.27	0.19

H17-23, Muscovite, 6.53 mg, J=0.0015471±0.02%, D=1±0, NM-303C, Lab#=66820-01

Cretaceous granite (N40.94286; W114.62854)

A	450.0	1213.4	0.4970	3712.6	0.2	1.0	9.6	0.2	303.09	11.22
B	500.0	279.3	0.6393	743.6	0.1	0.80	21.3	0.3	161.56	9.38
C	550.0	113.4	0.5817	253.3	0.2	0.88	34.0	0.4	106.25	4.77
D	590.0	51.47	0.7440	92.37	0.5	0.69	47.1	0.8	67.41	1.25
E	620.0	36.80	0.8145	44.44	0.6	0.63	64.5	1.3	66.03	0.91
F	650.0	32.79	0.5279	31.23	0.9	0.97	72.0	2.1	65.69	0.63
G	680.0	31.59	0.2523	28.27	1.3	2.0	73.6	3.2	64.71	0.42
H	700.0	30.87	0.1880	24.80	1.3	2.7	76.3	4.3	65.54	0.42
I	730.0	31.04	0.1562	22.27	2.2	3.3	78.8	6.1	68.03	0.27
J	750.0	30.13	0.1165	18.40	2.5	4.4	82.0	8.2	68.67	0.24
K	760.0	29.17	0.0994	13.45	2.4	5.1	86.4	10.2	70.01	0.26
L	770.0	29.50	0.1103	13.74	2.4	4.6	86.3	12.2	70.69	0.26
M	780.0	28.82	0.0714	11.14	2.7	7.1	88.6	14.5	70.91	0.21
N	790.0	28.36	0.0705	9.690	2.8	7.2	89.9	16.8	70.84	0.21
O	800.0	28.46	0.0513	9.665	3.1	9.9	90.0	19.5	71.12	0.18
P	810.0	28.61	0.0486	9.715	3.4	10.5	90.0	22.3	71.50	0.18
Q	820.0	29.06	0.0422	10.21	3.9	12.1	89.6	25.6	72.31	0.16
R	830.0	28.31	0.0335	7.706	4.3	15.2	92.0	29.2	72.28	0.14
S	840.0	28.41	0.0438	7.138	4.6	11.7	92.6	33.1	73.02	0.13
T	850.0	28.14	0.0283	6.277	4.5	18.0	93.4	36.9	72.97	0.13
U	860.0	28.10	0.0377	5.906	4.5	13.5	93.8	40.7	73.16	0.14
V	870.0	28.42	0.0436	6.182	4.4	11.7	93.6	44.3	73.81	0.14
W	890.0	28.53	0.0442	6.250	5.4	11.5	93.5	48.9	74.05	0.11
X	910.0	28.62	0.0393	6.395	6.1	13.0	93.4	54.0	74.19	0.11
Y	930.0	28.77	0.0387	6.778	6.2	13.2	93.0	59.2	74.28	0.11
Z	950.0	29.20	0.0415	7.335	5.4	12.3	92.6	63.8	75.00	0.12
AA	970.0	29.56	0.0478	7.801	5.0	10.7	92.2	68.0	75.61	0.13
AB	1000.0	29.75	0.0606	7.699	5.8	8.4	92.4	72.9	76.22	0.11
AC	1050.0	29.43	0.0572	7.077	10.1	8.9	92.9	81.4	75.84	0.07
AD	1100.0	29.29	0.0328	5.270	14.6	15.6	94.7	93.7	76.92	0.05
AE	1150.0	30.40	0.0581	5.491	1.5	8.8	94.7	94.9	79.74	0.41
AF	1250.0	74.28	0.3588	22.72	2.4	1.4	91.0	96.9	182.12	0.58
AG	1650.0	82.56	0.5256	124.6	3.7	0.97	55.5	100.0	125.35	0.35
Integrated age ± 2s			n=33			5.8			78.02	0.08
Isochron±2s		steps A-AG	n=33	MSWD=4949.73		$^{40}Ar/^{36}Ar=$	418.5±1.2		74.01	0.07

H18-23M, Muscovite, 7.89 mg, J=0.0015461±0.02%, D=1±0, NM-303C, Lab#=66822-01

Cretaceous granite (N40.930282; W114.64415)

A	450.0	244.6	0.0573	801.7	0.4	8.9	3.1	0.1	21.59	2.04
B	500.0	54.01	0.3523	137.0	0.2	1.4	25.1	0.2	37.97	2.03
C	550.0	35.69	0.1657	54.32	0.3	3.1	55.1	0.3	54.79	1.75
D	590.0	28.07	0.1474	24.11	0.4	3.5	74.7	0.4	58.38	1.13
E	620.0	26.51	0.0537	15.61	0.5	9.5	82.6	0.7	60.95	0.87
F	650.0	26.79	0.0407	14.96	0.8	12.5	83.5	0.9	62.26	0.64
G	680.0	26.73	0.0718	14.18	1.1	7.1	84.3	1.3	62.71	0.46
H	700.0	26.98	0.0173	14.97	1.2	29.4	83.6	1.8	62.74	0.43
I	730.0	27.37	-0.0023	16.04	1.9	-	82.7	2.5	62.96	0.28
J	750.0	26.74	0.0342	12.53	2.2	14.9	86.2	3.3	64.08	0.25
K	760.0	26.23	0.0232	10.09	2.1	22.0	88.6	4.1	64.66	0.25
L	770.0	25.63	0.0215	7.241	2.2	23.8	91.7	5.0	65.31	0.23
M	780.0	25.56	0.0190	6.006	2.6	26.8	93.1	5.9	66.11	0.22
N	790.0	25.11	0.0161	4.603	3.1	31.6	94.6	7.1	66.01	0.18
O	800.0	25.05	0.0161	3.908	3.8	31.8	95.4	8.5	66.42	0.14
P	810.0	24.79	0.0182	2.682	4.8	28.1	96.8	10.3	66.69	0.11
Q	820.0	24.84	0.0100	2.445	6.0	51.1	97.1	12.6	67.00	0.09
R	830.0	25.01	0.0102	2.837	7.2	50.0	96.7	15.3	67.17	0.08
S	840.0	24.95	0.0089	2.246	8.2	57.2	97.3	18.4	67.47	0.07
T	850.0	25.00	0.0029	1.208	11.1	178.3	98.6	22.6	68.44	0.05
U	860.0	24.82	0.0059	0.8980	11.7	85.9	98.9	27.0	68.22	0.05
V	870.0	33.43	0.0114	32.62	10.9	44.7	71.2	31.1	66.13	0.09
W	890.0	24.44	0.0054	0.7654	14.0	93.9	99.1	36.4	67.28	0.04
X	910.0	24.35	0.0071	0.8916	13.2	72.0	98.9	41.4	66.94	0.05
Y	930.0	24.38	0.0029	1.015	13.7	178.6	98.8	46.5	66.92	0.04
Z	950.0	24.37	0.0027	1.038	13.0	185.7	98.7	51.4	66.88	0.04
AA	970.0	24.48	0.0010	1.052	11.8	527.5	98.7	55.9	67.15	0.05
AB	1000.0	24.68	0.0048	1.065	13.3	106.2	98.7	60.9	67.69	0.05
AC	1050.0	24.99	0.0033	1.156	20.1	154.3	98.6	68.4	68.47	0.03
AD	1100.0	25.24	0.0013	0.8729	40.2	395.7	99.0	83.6	69.37	0.02
AE	1150.0	25.38	0.0007	0.6076	9.7	723.9	99.3	87.2	69.98	0.06
AF	1250.0	25.36	0.0040	0.6323	15.0	128.6	99.3	92.9	69.90	0.04
AG	1600.0	37.20	0.0052	39.46	18.9	98.8	68.7	100.0	70.88	0.07
Integrated age ± 2s			n=33			75.7			67.87	0.04
Isochron±2s		steps A-AG	n=33	MSWD=488.49		$^{40}Ar/^{36}Ar$=	297.9±0.9		68.37	0.04

H18-24, Muscovite, 4.41 mg, J=0.0015295±0.02%, D=1±0, NM-303C, Lab#=66824-01

Cambrian-Neoproterozoic Prospect Mountain Quartzite (N40.930476; W114.64437)

A	450.0	215.9	0.1319	705.0	0.2	3.9	3.5	0.2	21.23	2.50
B	500.0	110.2	-0.2575	325.0	0.1	-	12.8	0.2	39.15	5.69
C	550.0	38.11	0.0263	70.46	0.2	19.4	45.4	0.4	47.77	2.37
D	590.0	27.79	-0.0291	34.27	0.2	-	63.5	0.5	48.78	2.31
E	620.0	26.88	0.0613	18.48	0.4	8.3	79.7	0.9	59.01	1.21
F	650.0	24.77	0.0707	11.43	0.5	7.2	86.4	1.3	58.96	0.97
G	680.0	23.59	-0.0387	7.579	0.7	-	90.5	1.9	58.80	0.65
H	700.0	23.71	0.0004	5.076	0.7	1163.0	93.7	2.5	61.16	0.65
I	730.0	23.93	0.0168	4.814	1.1	30.3	94.1	3.5	61.95	0.41
J	750.0	23.51	0.0267	3.712	1.2	19.1	95.3	4.6	61.69	0.40
K	760.0	23.77	0.0084	3.782	1.1	60.7	95.3	5.6	62.35	0.44
L	770.0	23.87	0.0030	3.471	1.0	170.0	95.7	6.5	62.86	0.45
M	780.0	24.30	-0.0097	4.045	1.2	-	95.1	7.5	63.58	0.41
N	790.0	25.49	-0.0081	5.188	1.4	-	94.0	8.7	65.86	0.38
O	800.0	25.40	0.0334	4.547	1.6	15.3	94.7	10.2	66.14	0.31

H18-24 (continued)

P	810.0	25.59	0.0041	3.282	1.9	124.5	96.2	11.9	67.66	0.28
Q	820.0	25.98	-0.0240	3.552	2.2	-	96.0	13.8	68.49	0.25
R	830.0	25.85	0.0000	2.710	2.6	10718.6	96.9	16.1	68.82	0.20
S	840.0	25.96	-0.0090	2.055	3.0	-	97.7	18.8	69.63	0.17
T	850.0	25.83	-0.0158	1.489	3.3	-	98.3	21.8	69.73	0.16
U	860.0	25.81	-0.0141	1.307	3.5	-	98.5	24.9	69.83	0.16
V	870.0	25.82	-0.0035	1.288	3.6	-	98.5	28.1	69.88	0.15
W	890.0	25.56	-0.0028	1.116	5.5	-	98.7	33.0	69.29	0.11
X	910.0	25.31	-0.0009	1.029	6.8	-	98.8	39.0	68.72	0.08
Y	930.0	25.09	-0.0052	1.198	8.8	-	98.6	46.8	67.98	0.06
Z	950.0	25.33	-0.0045	1.199	10.1	-	98.6	55.8	68.61	0.06
AA	970.0	25.72	-0.0001	1.117	9.5	-	98.7	64.2	69.74	0.06
AB	1000.0	26.17	-0.0012	1.114	10.3	-	98.7	73.5	70.96	0.06
AC	1050.0	26.72	-0.0032	1.009	13.1	-	98.9	85.1	72.53	0.05
AD	1100.0	27.33	0.0025	1.152	9.1	204.8	98.8	93.2	74.04	0.07
AE	1150.0	27.75	-0.0132	2.060	1.0	-	97.8	94.2	74.44	0.54
AF	1250.0	28.74	0.0242	5.184	1.2	21.1	94.7	95.2	74.63	0.44
AG	1650.0	67.74	0.0204	135.6	5.3	25.0	40.9	100.0	75.89	0.24
Integrated age ± 2s			n=33			-795.481			69.69	0.07
Isochron±2s		steps A-AG	n=33	MSWD=382.59		$^{40}Ar/^{36}Ar$=	304.7±1.2		70.47	0.05

H18-40, Muscovite, 4.27 mg, J=0.0015208±0.03%, D=1±0, NM-303C, Lab#=66825-01

Cretaceous granite dike (N40.93581; W114.63277)

A	550.0	30.15	-0.0357	32.76	0.2	-	67.9	0.2	56.11	1.84
B	590.0	25.79	0.2110	17.51	0.4	2.4	80.0	0.4	56.57	1.15
C	620.0	26.28	0.2781	13.94	0.5	1.8	84.4	0.8	60.76	0.96
D	650.0	25.83	0.2835	10.85	0.7	1.8	87.7	1.3	62.01	0.72
E	680.0	25.77	0.2118	7.981	0.9	2.4	90.9	2.0	64.09	0.53
F	700.0	26.50	0.0231	8.699	1.0	22.0	90.3	2.7	65.45	0.47
G	730.0	27.93	0.0141	11.06	1.6	36.2	88.3	3.9	67.40	0.33
H	750.0	28.53	0.0033	10.92	1.9	155.4	88.7	5.3	69.11	0.29
I	760.0	28.75	0.0143	9.360	1.6	35.7	90.4	6.5	70.95	0.32
J	770.0	28.75	0.0166	8.602	1.7	30.8	91.2	7.7	71.54	0.34
K	780.0	28.67	0.0241	6.716	1.9	21.1	93.1	9.1	72.83	0.28
L	790.0	28.08	0.0195	5.247	2.3	26.1	94.5	10.8	72.42	0.24
M	800.0	27.67	0.0163	3.945	2.6	31.3	95.8	12.8	72.33	0.21
N	810.0	27.72	0.0116	4.155	3.1	43.9	95.6	15.1	72.30	0.18
O	820.0	27.43	0.0140	3.572	3.7	36.5	96.2	17.8	72.00	0.15
P	830.0	27.48	0.0106	2.954	4.2	48.1	96.8	20.9	72.62	0.13
Q	840.0	27.90	0.0034	2.643	7.1	149.4	97.2	26.1	73.97	0.09
R	850.0	27.40	0.0056	1.305	7.5	90.6	98.6	31.6	73.71	0.08
S	860.0	27.09	0.0095	1.271	6.2	53.6	98.6	36.1	72.89	0.09
T	870.0	26.89	0.0152	1.312	5.6	33.5	98.6	40.3	72.33	0.10
U	890.0	26.82	0.0034	1.522	6.5	149.2	98.3	45.1	71.97	0.09
V	910.0	26.80	0.0026	1.478	6.6	194.7	98.4	50.0	71.96	0.09
W	930.0	26.77	0.0088	1.763	6.7	57.9	98.1	54.9	71.66	0.08
X	950.0	26.94	0.0074	2.301	5.9	69.3	97.5	59.3	71.68	0.10
Y	970.0	27.07	0.0063	2.189	5.5	81.6	97.6	63.4	72.12	0.10
Z	1000.0	27.37	0.0018	2.324	5.6	278.5	97.5	67.5	72.81	0.10
AA	1050.0	27.80	0.0031	2.430	9.1	162.7	97.4	74.3	73.88	0.07
AB	1100.0	28.09	0.0059	2.161	12.9	86.5	97.7	83.8	74.86	0.05
AC	1150.0	28.31	0.0129	2.766	2.5	39.5	97.1	85.6	74.97	0.25
AD	1250.0	28.30	0.0030	1.743	13.9	170.4	98.2	95.8	75.77	0.05
AE	1650.0	53.10	0.0088	84.23	5.6	58.3	53.1	100.0	76.88	0.18
Integrated age ± 2s			n=31			43.8			72.98	0.06
Isochron±2s		steps A-AE	n=31	MSWD=247.95		$^{40}Ar/^{36}Ar$=	306.9±1.7		73.60	0.06

61418(2), Muscovite, 4.16 mg, J=0.0014901±0.02%, D=1±0, NM-303C, Lab#=66829-01

Cambrian Morgan Pass Formation, biotite-muscovite schist (N40.974632; W114.60786)

A	500.0	137.7	-0.0636	388.2	0.2	-	16.7	0.1	61.70	3.28
B	550.0	40.29	-0.2528	47.72	0.1	-	64.9	0.2	70.00	4.62
C	590.0	32.12	0.1663	21.95	0.2	3.1	79.8	0.4	68.67	2.32
D	620.0	32.32	0.2481	13.83	0.3	2.1	87.4	0.6	75.49	1.61
E	650.0	30.09	0.1453	7.765	0.5	3.5	92.4	1.0	74.32	0.95
F	680.0	29.86	0.0199	6.376	0.9	25.7	93.7	1.7	74.76	0.63
G	700.0	29.11	0.0197	4.539	1.0	25.9	95.4	2.5	74.21	0.52
H	730.0	29.31	0.0004	4.061	1.6	1326.9	95.9	3.6	75.12	0.36
I	750.0	29.31	-0.0185	3.045	1.7	-	96.9	4.9	75.90	0.34
J	760.0	29.06	0.0069	2.916	1.4	74.2	97.0	6.0	75.34	0.37
K	770.0	29.66	0.0080	4.143	1.3	64.1	95.9	7.0	75.97	0.39
L	780.0	29.86	-0.0014	4.021	1.3	-	96.0	8.0	76.59	0.43
M	790.0	29.77	0.0050	4.992	1.4	102.5	95.0	9.1	75.59	0.38
N	800.0	30.91	0.0107	7.282	1.7	47.7	93.0	10.4	76.81	0.34
O	810.0	31.03	0.0027	5.152	2.7	186.2	95.1	12.5	78.78	0.22
P	820.0	31.01	0.0004	3.972	4.3	1185.1	96.2	15.7	79.62	0.14
Q	830.0	30.29	0.0071	2.050	5.6	72.1	98.0	20.0	79.22	0.11
R	840.0	30.00	0.0035	1.387	5.8	144.7	98.6	24.4	78.98	0.11
S	850.0	29.69	-0.0124	1.104	5.3	-	98.9	28.4	78.40	0.11
T	860.0	29.67	-0.0096	1.204	4.5	-	98.8	31.8	78.25	0.13
U	870.0	29.76	0.0002	1.249	4.3	2370.8	98.8	35.0	78.47	0.13
V	890.0	29.68	0.0022	1.299	5.2	227.2	98.7	39.0	78.23	0.11
W	910.0	29.61	-0.0007	1.587	5.6	-	98.4	43.2	77.82	0.10
X	930.0	29.37	0.0035	1.683	5.8	144.6	98.3	47.7	77.10	0.10
Y	950.0	29.27	0.0019	1.837	6.0	262.5	98.1	52.2	76.74	0.10
Z	970.0	29.04	0.0018	1.749	6.6	279.1	98.2	57.3	76.19	0.09
AA	1000.0	28.84	0.0056	1.351	9.4	91.6	98.6	64.4	75.99	0.06
AB	1050.0	29.70	0.0039	1.449	12.1	131.7	98.6	73.6	78.16	0.05
AC	1100.0	30.63	0.0023	1.165	23.1	224.8	98.9	91.2	80.81	0.03
AD	1150.0	30.83	-0.0018	1.001	3.4	-	99.0	93.8	81.45	0.17
AE	1250.0	31.18	0.0185	2.222	4.0	27.5	97.9	96.8	81.41	0.16
AF	1650.0	86.51	0.0558	182.2	4.2	9.1	37.8	100.0	87.04	0.32
Integrated age ± 2s			n=32			98.7			78.59	0.06
Isochron±2s		steps A-AF	n=32	MSWD=290.70		$^{40}Ar/^{36}Ar$=	311.0±1.4		78.92	0.05

H15-35, Muscovite, 1.26 mg, J=0.0014996±0.02%, D=1±0, NM-303C, Lab#=66827-01

Cambrian Dunderberg Shale, biotite-muscovite schist (N40.936114; W114.62515)

A	0.4	41.63	2.896	110.1	0.2	0.18	22.4	2.7	25.46	1.16
B	0.6	25.29	6.359	19.72	0.2	0.080	79.0	5.4	54.24	1.80
C	0.8	26.74	4.660	9.253	0.4	0.11	91.2	10.0	65.94	1.24
D	1.0	27.66	2.010	4.738	0.6	0.25	95.5	17.6	71.23	0.77
E	1.2	27.88	1.200	3.581	0.8	0.43	96.6	27.3	72.51	0.62
F	1.5	28.20	0.6838	3.189	1.2	0.75	96.8	41.7	73.51	0.43
G	2.0	28.80	0.4514	2.926	1.9	1.1	97.1	65.0	75.25	0.30
H	3.0	29.83	0.4679	2.365	1.9	1.1	97.8	89.0	78.38	0.29
I	4.0	32.06	0.9744	2.184	0.6	0.52	98.2	95.9	84.54	1.01
J	5.0	34.93	1.124	3.265	0.1	0.45	97.5	97.8	91.25	4.23
K	8.0	47.13	2.592	5.441	0.1	0.20	97.0	99.1	121.62	7.22
L	15.0	59.56	2.681	9.660	0.1	0.19	95.6	100.0	150.19	14.32
Integrated age ± 2s			n=12			0.43			75.09	0.45
Isochron±2s		steps A-L	n=12	MSWD=50.62		$^{40}Ar/^{36}Ar$=	100.1±7.8		77.67	0.38

H18-40, K-Feldspar, 16.07 mg, J=0.0015541±0.02%, D=1±0, NM-303F, Lab#=66862-01

Cretaceous granite dike (N40.93581; W114.63277)

A	500.0	275.7	0.0077	739.1	13194.0	66.7	20.8	0.3	156.17	0.76
B	500.0	25.67	-0.0164	37.41	22626.4	-	56.9	0.9	41.09	0.14
C	550.0	16.75	0.0067	16.08	3546.5	76.1	71.6	1.0	33.81	0.41
D	550.0	13.51	0.0030	4.861	70896.2	171.5	89.4	2.8	34.02	0.03
E	600.0	13.57	0.0031	3.368	73760.9	163.4	92.7	4.7	35.42	0.03
F	600.0	13.09	0.0041	1.771	105821.3	125.4	96.0	7.4	35.40	0.02
G	650.0	13.54	0.0071	1.685	102994.1	71.9	96.3	10.0	36.72	0.02
H	650.0	13.35	0.0038	1.045	126883.0	134.6	97.7	13.2	36.74	0.02
I	700.0	13.65	0.0006	1.038	94735.0	814.5	97.8	15.6	37.58	0.02
J	700.0	13.67	0.0000	0.8417	137152.0	46382.2	98.2	19.1	37.79	0.01
K	750.0	13.88	0.0041	0.8460	86163.2	124.5	98.2	21.2	38.37	0.02
L	750.0	13.90	-0.0026	0.6160	113597.3	-	98.7	24.1	38.62	0.02
M	800.0	14.09	0.0012	0.5872	79612.2	420.1	98.8	26.1	39.17	0.02
N	800.0	14.20	-0.0018	0.5218	97513.8	-	98.9	28.6	39.54	0.02
O	850.0	14.46	-0.0021	0.6609	81081.2	-	98.6	30.7	40.13	0.02
P	850.0	14.54	0.0002	0.5365	100348.2	2338.2	98.9	33.2	40.47	0.02
Q	900.0	14.78	0.0000	0.6472	87078.1	20996.0	98.7	35.4	41.03	0.02
R	900.0	14.87	-0.0044	0.4938	107298.4	-	99.0	38.2	41.42	0.02
S	950.0	15.12	0.0033	0.7049	80905.8	156.9	98.6	40.2	41.95	0.02
T	950.0	15.30	0.0003	0.5818	109997.4	1591.4	98.9	43.0	42.55	0.02
U	1000.0	15.78	0.0013	1.026	79782.1	398.6	98.1	45.0	43.52	0.03
V	1000.0	16.13	0.0001	1.304	99955.7	6951.0	97.6	47.6	44.26	0.02
W	1050.0	16.89	0.0023	2.463	69408.7	219.0	95.7	49.3	45.40	0.03
X	1050.0	16.84	0.0024	1.373	97094.6	212.2	97.6	51.8	46.15	0.02
Y	1100.0	17.73	0.0023	2.084	78217.7	222.6	96.5	53.8	48.06	0.03
Z	1100.0	17.82	0.0002	2.098	108794.8	2095.3	96.5	56.5	48.30	0.02
BA	1150.0	18.26	0.0035	2.559	91981.8	146.8	95.9	58.8	49.13	0.03
BB	1150.0	18.15	0.0014	2.430	132793.7	352.9	96.0	62.2	48.94	0.02
BC	1150.0	18.39	0.0021	3.090	243685.4	248.4	95.0	68.4	49.05	0.02
BD	1150.0	19.10	-0.0002	4.793	265468.8	-	92.6	75.1	49.62	0.02
BE	1200.0	20.22	-0.0093	6.507	19091.3	-	90.5	75.6	51.33	0.12
BF	1250.0	19.53	-0.0025	5.581	123739.6	-	91.6	78.8	50.18	0.03
BG	1300.0	20.73	0.0003	7.691	519582.5	1547.9	89.0	91.9	51.77	0.01
BH	1500.0	26.42	0.0011	28.38	298988.3	473.5	68.3	99.5	50.60	0.03
BI	1650.0	367.7	0.0054	1193.5	19252.2	93.7	4.1	100.0	42.30	0.75
Integrated age ± 2s			n=35			601.8			45.13	0.02
Isochron±2s		steps A-BI	n=35	MSWD=36342.52		$^{40}Ar/^{36}Ar$=	525.9±0.6		41.31	0.02

H18-23, K-Feldspar, 14.38 mg, J=0.0015142±0.03%, D=1±0, NM-303F, Lab#=66866-01

Cretaceous granite (N40.930282; W114.64415)

A	500.0	167.3	-0.0023	341.6	13148.9	-	39.7	0.4	175.33	0.64
B	500.0	24.78	-0.0096	46.85	10938.3	-	44.1	0.7	30.05	0.21
C	550.0	15.75	0.0100	15.66	25448.4	51.1	70.6	1.5	30.57	0.09
D	550.0	13.38	0.0003	7.356	41913.9	1954.1	83.8	2.7	30.81	0.05
E	600.0	14.07	0.0016	4.851	61044.6	328.4	89.8	4.5	34.68	0.03
F	600.0	13.58	0.0050	3.014	79999.6	101.8	93.4	6.9	34.84	0.03
G	650.0	13.77	0.0028	2.487	98642.5	180.7	94.7	9.8	35.79	0.02
H	650.0	13.42	0.0004	1.296	117841.8	1232.7	97.1	13.3	35.78	0.02
I	700.0	13.71	0.0006	1.373	117403.6	851.2	97.0	16.8	36.50	0.02
J	700.0	13.64	0.0037	0.8099	140892.2	137.4	98.2	21.0	36.78	0.02
K	750.0	13.94	0.0019	1.135	116451.3	266.9	97.6	24.5	37.33	0.02
L	750.0	13.95	0.0030	0.7950	112371.7	167.7	98.3	27.8	37.63	0.02

H18-23 (continued)

M	800.0	14.19	0.0006	0.9068	78811.7	802.2	98.1	30.2	38.19	0.02
N	800.0	14.33	0.0015	1.156	91842.0	341.6	97.6	32.9	38.36	0.02
O	850.0	14.40	0.0042	0.8694	73956.1	121.9	98.2	35.1	38.78	0.03
P	850.0	14.43	0.0000	0.7885	92968.5	-	98.4	37.9	38.94	0.02
Q	900.0	14.67	-0.0040	1.046	77824.6	-	97.9	40.2	39.37	0.03
R	900.0	14.64	0.0044	0.7340	102408.0	115.2	98.5	43.2	39.53	0.02
S	950.0	15.05	0.0015	1.477	68155.5	337.0	97.1	45.2	40.06	0.03
T	950.0	15.11	0.0013	1.122	68581.6	390.4	97.8	47.3	40.52	0.03
U	1000.0	15.70	0.0039	2.534	48383.5	131.0	95.2	48.7	40.98	0.04
V	1000.0	16.00	0.0072	2.809	51204.5	71.1	94.8	50.2	41.57	0.04
W	1050.0	16.51	0.0116	4.272	45450.5	44.1	92.4	51.6	41.79	0.05
X	1050.0	16.77	0.0063	4.388	58697.9	81.4	92.3	53.3	42.41	0.04
Y	1100.0	17.37	0.0132	5.539	50113.1	38.8	90.6	54.8	43.10	0.05
Z	1100.0	17.30	0.0109	4.858	71292.7	47.0	91.7	56.9	43.45	0.04
BA	1150.0	17.93	0.0108	6.175	61767.0	47.4	89.8	58.8	44.10	0.04
BB	1150.0	17.79	0.0057	6.041	94631.0	90.1	90.0	61.6	43.83	0.03
BC	1150.0	17.73	0.0028	5.661	177719.0	179.4	90.6	66.9	43.97	0.02
BD	1150.0	18.14	0.0022	6.636	204137.9	234.0	89.2	72.9	44.30	0.02
BE	1200.0	18.23	0.0024	6.106	13183.9	216.3	90.1	73.3	44.97	0.15
BF	1300.0	17.97	-0.0512	6.266	11814.7	-	89.7	73.7	44.12	0.17
BG	1300.0	18.93	0.0005	6.320	716918.1	985.3	90.1	95.0	46.69	0.01
BH	1500.0	28.31	0.0032	38.33	147383.7	160.4	60.0	99.4	46.48	0.05
BI	1650.0	213.5	-0.0177	671.2	20693.0	-	7.1	100.0	41.65	0.56
Integrated age ± 2s			n=35			217.9			41.89	0.02
Isochron±2s		steps A-BI	n=35	MSWD=13134.11		$^{40}Ar/^{36}Ar$=	483.2±0.7		38.21	0.02

Notes:

Isotopic ratios corrected for blank, radioactive decay, and mass discrimination, not corrected for interfering reactions.

Errors quoted for individual analyses include analytical error only, without interfering reaction or J uncertainties.

Integrated age calculated by summing isotopic measurements of all steps.

Integrated age error calculated by quadratically combining errors of isotopic measurements of all steps.

Plateau age is inverse-variance-weighted mean of selected steps.

Plateau age error is inverse-variance-weighted mean error (Taylor, 1982) times root MSWD where MSWD>1.

Plateau error is weighted error of Taylor (1982).

Decay constants and isotopic abundances after Steiger and Jäger (1977).

Ages calculated relative to FC-2 Fish Canyon Tuff sanidine interlaboratory standard at 28.201 Ma after Kuiper et al.(2008)

Decay Constant (LambdaK (total)) = 5.463e-10/a

Correction factors:

$(^{39}Ar/^{37}Ar)_{Ca}$ = 0.0006926 ± 0.000016

$(^{36}Ar/^{37}Ar)_{Ca}$ = 0.0002702 ± 0.0000010

$(^{38}Ar/^{39}Ar)_{K}$ = 0.0121

$(^{40}Ar/^{39}Ar)_{K}$ = 0.000129 ± 8e-05